Air-to-air atmospheric pressure plasma treatment – perspective for composite manufacturing

Cheng Fang[1,2], Daan Jonas Hottentot Cederløf[1], Alexander Bardenshtein[3] and Yukihiro Kusano[1,3*]

[1] Department of Wind Energy, Technical University of Denmark, Denmark
[2] Harbin Institute of Technology, People's Republic of China
[3] Danish Technological Institute, Denmark

*: corresponding author
e-mail: yuk@teknologisk.dk

Abstract. Fibre-reinforced polymer composites are gaining increasing attention in various applications for constructing mechanical structures such as wind turbine blades. The interface between fibres and a polymer matrix should be optimally designed to promote the mechanical performance of the composites. Plasma treatment shows obvious advantages over conventional approaches, since it has the characteristic of environmental friendliness, low-cost, and easy operation. A plasma can be favourably generated at atmospheric pressure. One of the most commonly used atmospheric pressure plasmas is a dielectric barrier discharge (DBD). In the present work, an air-to-air DBD is introduced. The DBD was generated in a gas mixture of helium and fluorocarbon between a rod-shaped water-cooled powered electrode covered with alumina and a one-dimensionally movable ground aluminium plate. Polyethylene terephthalate films were used as model specimens, and attached on the aluminium plate for the surface modification. The results indicate that specimen surfaces can be oxidized or fluorinated, depending on the conditions, and that the gap between the electrodes and gas flowrates significantly affect the treatment effect.

1. Introduction

Glass fibre reinforced polymer (GFRP) composites are widely used due to high strength-to-weight ratios, mechanical and corrosion resistance properties [1]. Examples of applications include sporting equipment, vehicles, architectures, and wind turbine blades.

It is indicated experimentally [2] and theoretically [3] that fracture toughness of GFRPs can be improved not by strong interactions at the interfaces between fibres and polymer matrices, but by optimally designed interfaces. More specifically, creation of multiple cracks in GFRPs due to locally distributed domains with low adhesion can improve overall fracture toughness of GFRPs. Therefore, at the initial stage of polymer composite manufacturing, surface treatment of fibres is important for controlling the interfacial properties of GFRPs. Motivated by this idea, fluorination of sized glass fibres is studied aiming at reducing initial interaction of glass fibre surfaces with polymer matrices [4,5]. Specifically, it is expected that fluorination of sized glass fibre surfaces can pronounce de-wetting of uncured matrix polymers, delay interaction between the sizing and the matrix, and that subsequent interfacial interaction can be lowered. Among the reported surface treatment techniques, atmospheric pressure plasma treatment is attractive due to its high treatment efficiency, environmental friendliness

and easy operation with simple setups [6,7]. Commonly used atmospheric pressure plasmas include corona discharge, dielectric barrier discharge (DBD) [8], cold plasma torch [9,10], and gliding arc [11-17]. DBD is generated by applying an alternating-current (AC) voltage between electrodes separated by one or more dielectrics. Simple and robust configuration of the DBD allows for design flexibility including air-to-air type continuous plasma treatment systems [18,19].

Adhesion improvement of material surfaces using plasma treatment [6,7] is commonly demonstrated by oxidation for acid-based interactions [20] and/or surface roughening for mechanical interlocking effects for the purpose of improving interactions at interfaces. By contrast, recent publications [4,5] propose designed lower interactions between glass fibre fabrics with a polymer matrix by creating a polytetrafluoroethylene (PTFE) like surface by substitution reactions between hydrogen and fluorine using a DBD in a helium/tetrafluoromethane (He/CF_4) gas mixture. However, it is reported that use of fluorocarbons such as hexafluoropropylene (HFP. C_3F_6) and octafluorocyclobutane (OFB. c-C_4F_8) in a DBD exhibits better hydrophobic effects by plasma polymerization to synthesize a PTFE like coating than use of CF_4 [21]. It is noted here that if plasma polymerization on a material surface is appropriately carried out, the surface property of the coating is generally independent of the material to be coated.

In the present work, an air-to-air DBD is introduced for investigating hydrophobic plasma surface modification in a He/OFB gas mixture. Polyethylene terephthalate (PET) films were used as model specimens to study the modification effects, since PET is easily available, and its properties are well-known. Contact angle measurements were carried out using deionized water and glycerol as test liquids for studying wetting characteristics. X-ray photoelectron spectroscopy (XPS) was used to characterize the elemental analysis of the modified PET film surfaces.

2. Experimental methods

A photo image and a diagram of the DBD setup are shown in Fig. 1. The powered electrode is water-cooled cylindrical metallic tube covered with an alumina tube. Inner and outer diameters of the alumina tube are 12 and 16 mm, respectively. The lower ground electrode is an aluminium plate (280 mm x 400 mm). The gap between the alumina tube and the aluminium plate was adjusted to 0.6 mm or 2.0 mm. He and OFB were used as a dilute gas and a reactive gas, respectively. A flowrate of He was adjusted between 14.5 and 29 standard litre per minute (SLM). OFB flowrate was adjusted between 0.066 and 0.262 SLM. A gas mixing ratio (MR) is defined in equation (1).

$$MR = F_{OFB} / (F_{He} + F_{OFB}) \times 100 \text{ (vol. \%)}, \quad (1)$$

where F_{OFB} and F_{He} are the flowrates of OFB and He, respectively.

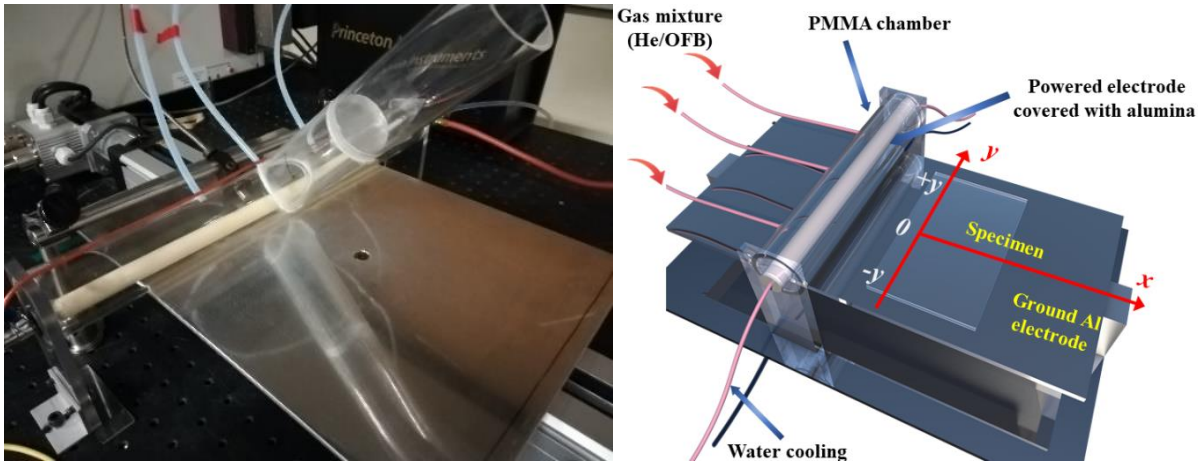

Fig. 1 A photo image and a diagram of the air-to-air atmospheric pressure DBD setup.

He gas was pre-mixed with OFB, and then introduced into a poly-methyl-methacrylate (PMMA) chamber, separating the gas mixture from the surrounding atmosphere. The bottom part of the PMMA chamber facing the aluminium plate is open to air so that the DBD was generated between the alumina tube and the aluminium plate. The DBD was driven by an AC power supply (Generator 6030, SOFTAL Electronic GmbH, Germany) at a frequency of approximately 40 kHz. Untreated general-purpose PET films with thickness of 65 μm were used as specimens. They were attached on the aluminium plate at positions in a y-axis direction of "-y" (approximately 5 cm from the edge of the aluminium plate), "0" (centre) and "+y" (approximately 5 cm from the edge of the aluminium plate). The aluminium plate was moved forward and backward in an x-axis direction at a speed ranging from 1 to 100 mm/s. The specimens were exposed to the DBD once or four times. The average power input was obtained by measuring voltage and current with a high-voltage probe and a 10 Ω current viewing resistor, respectively. The power of each treatment was adjusted to 100 W.

Static contact angles of deionized water and glycerol on the PET films before and after the treatment were measured in air at room temperature using a contact angle measurement system (CAM100; Crelab Instruments AB, Sweden). Here, deionized water is characterized by its significantly polar nature, and is the most commonly used test liquid for the contact angle measurement. Glycerol is also often used as a test liquid, exhibiting both polar and non-polar nature with high viscosity. Glycerol is considered to be an appropriate test liquid for screening adhesion properties of polymer surfaces due to similarities of physical properties to general adhesives and uncured resins [22].

XPS data were collected using a monochromatic Al K_α X-ray source with a lateral resolution of 30 mm (K-alpha; ThermoFischer Scientific, UK) to study the changes of the elemental composition at the PET film surfaces. Atomic concentrations of each element were calculated by determining the relevant integral peak intensities subtracting a linear background.

3. Results

A photo image of the DBD in the He/OFB gas mixture is exemplified in Fig. 2. The discharge looks a mixture of filamentary and glow-like discharges. It was confined between the electrodes, and spread along the powered electrode in the y-axis direction. The photoemission on the right side in Fig. 2, corresponding to +y direction, was more intense than at the centre and at the left-hand side. The difference of the photoemission is related to the uniformity of the plasma and treatment, which will be discussed below.

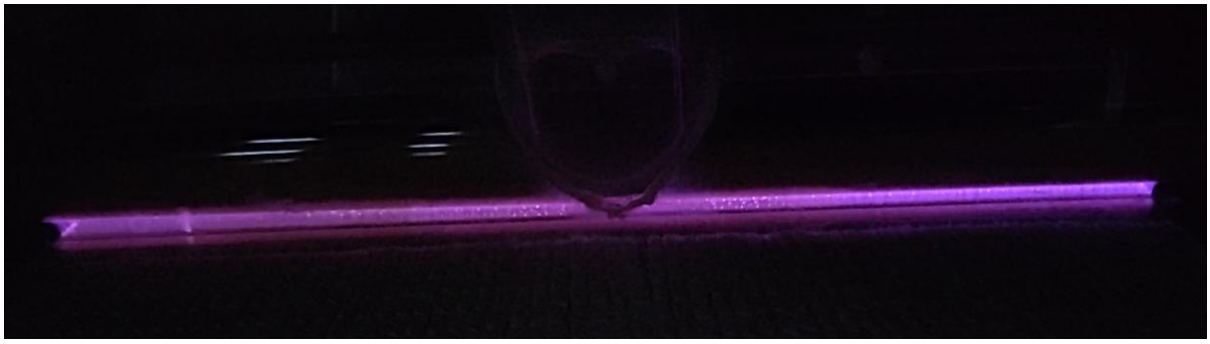

Fig. 2. A photo of the DBD in He/OFB gas mixture (gap: 2.0 mm, MR value: 0.45 %). The purple colour indicates photo-emission from the DBD between the cylindrical powered electrode and the ground electrode.

The voltage and current waveforms of the DBD in the He/OFB gas mixture are shown in Fig. 3. The voltage waveform was sinusoidal. The phase shift was approximately π/4, indicating that the DBD is

primarily a capacitively coupled plasma. Generation of the DBD in each half period deformed the current waveform from the sinusoidal feature.

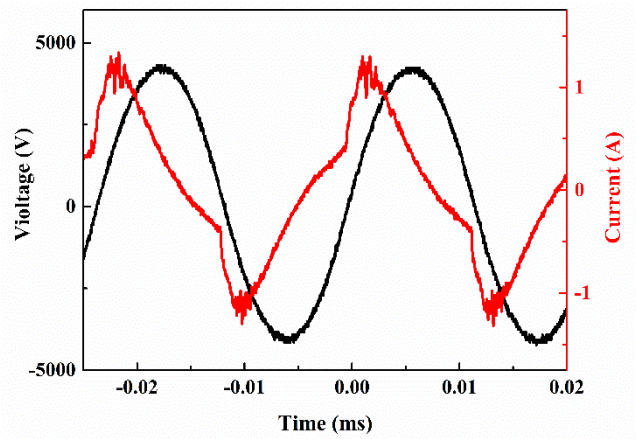

Fig. 3. An example of voltage (black) and current (red) waveforms of the DBD in He/OFB gas mixture (gap: 2.0 mm, MR value: 0.45 %).

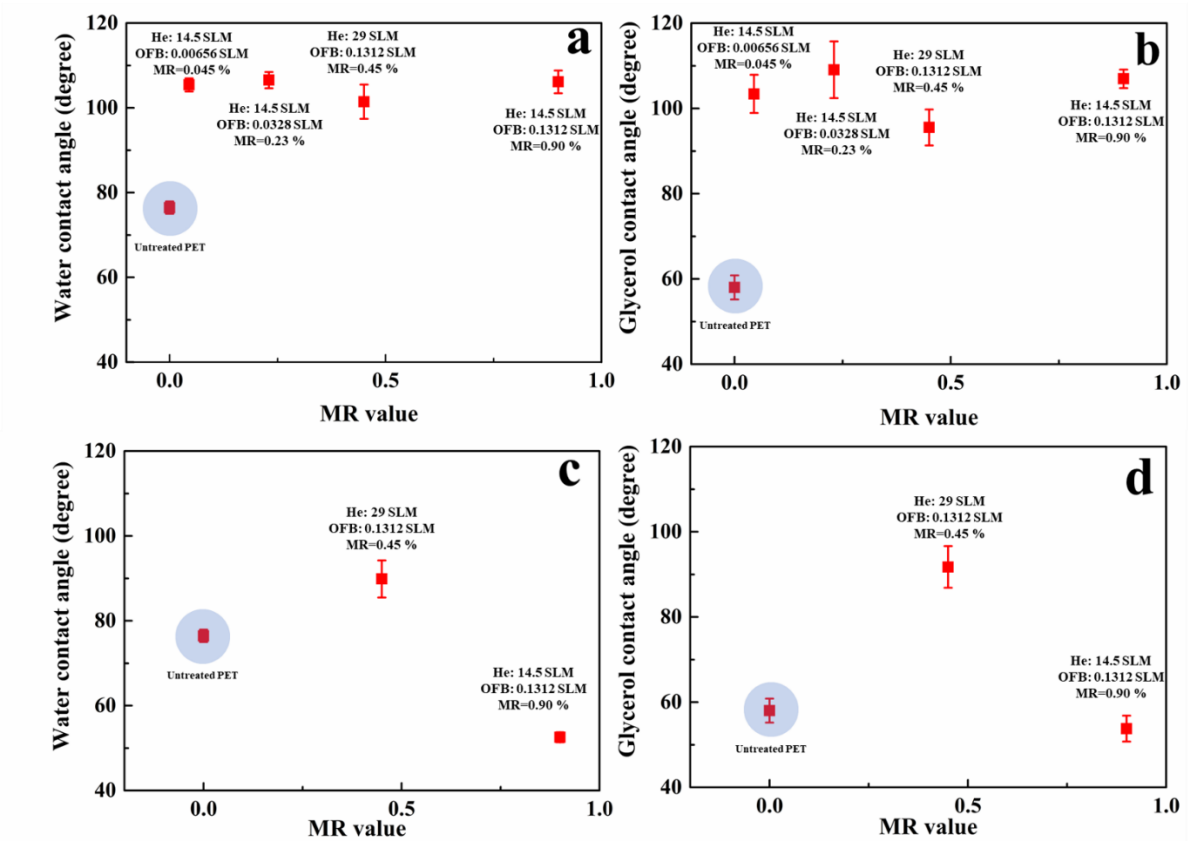

Fig. 4. Contact angles of deionized water and glycerol with the gaps of 0.6 mm (a, b) and 2.0 mm (c,d). (exposure: 4 times, MR value: 0.045 %, 0.23 %, 0.45 %, and 0.90 %). The contact angles for the untreated PET are also plotted in each figure.

In order to investigate the influence of different plasma process parameters on the wettability of the PET surfaces, static contact angles of deionized water and glycerol were measured after treatment. PET films without treatment were also tested for comparison and the values for deionized water and glycerol were 76.4 ± 1.5 and 58.0 ± 2.8 degrees, respectively. The gas content in a plasma is an important parameter for atmospheric pressure plasma processing. It depends on flowrates of the gases, the MR value, introduction of air from the surrounding, and consumption of the reactive gas by polymerization and/or decomposition in the plasma. The gap between the two electrodes, which affects the introduction of atmospheric air into the DBD, was first set to the minimum value of 0.6 mm. The MR value was set to 0.045 %, 0.23 %, 0.45 %, or 0.90 %. PET films were placed at the "0" position on the aluminium plate (see Fig. 1) and exposed to the DBD four times. Results of the contact angle measurement of the PET films treated under different conditions are summarized in the Fig. 4 (a,b). The contact angle increased greatly after each treatment.

Next, the gap was set to 2.0 mm and similar experiments were carried out. Fig. 4 (c,d) illustrates the results of the contact angle measurement, showing a different trend from the smaller gap in Fig. 4 (a,b). When the MR value was set from 0.045 to 0.45 %, the contact angles of deionized water and glycerol increased, but were lower than the values achieved at the gap of 0.6 mm. When the MR value was 0.9 % by decreasing the He flowrate from 29 SLM to 14.5 SLM, the contact angles were even lower than those of the original PET films.

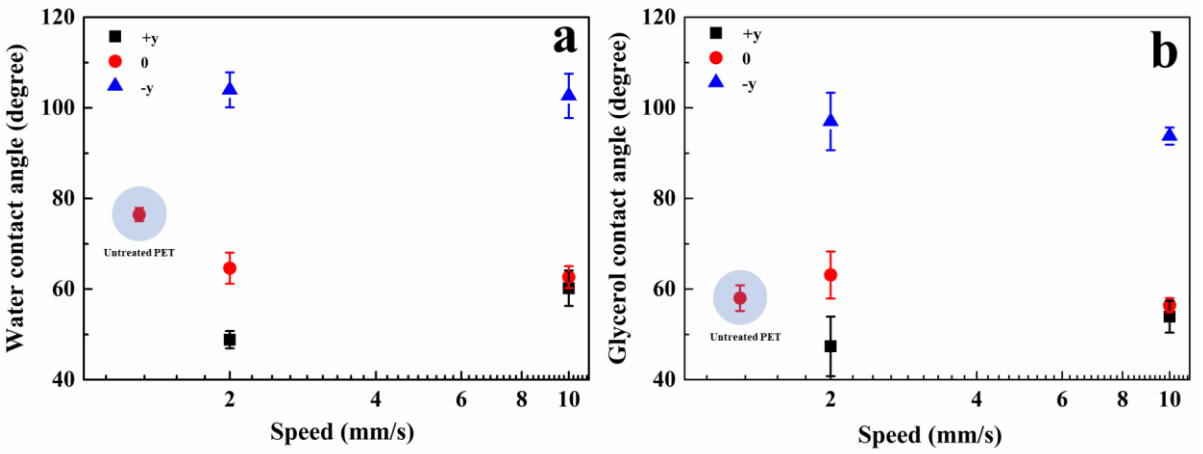

Fig. 5. Contact angles at position of –y, 0, and +y. (a) deionized water, (b) glycerol (exposure: once, gap: 2.0 mm, MR value: 0.45 %, He flowrate: 29 SLM). The contact angles for the untreated PET are also plotted in each figure.

Since the DBD can treat an up to A4 size specimen (210 mm x 300 mm), it is worth investigating the treatment uniformity. In addition, time for treatment is an important parameter for practical applicability of the processing. It can be changed by the number of the exposures and the moving speed of the aluminium plate. In the following experiments, the number of exposures is fixed to one time. In addition, the PET films were fixed at the positions of "-y", "0" and "+y", the moving speed was varied between 1 and 100 mm/s, and the gap and the He flowrate were fixed at 2.0 mm and 29 SLM, respectively.

The MR value was fixed at 0.45 %, and contact angles of deionized water and glycerol were measured after the treatments as shown in Fig. 5. The result indicates that the treatment was significantly uneven. The "-y" position became highly hydrophobic. On the other hand, at the "0" and "+y" positions, the water contact angle was slightly lowered from the original value of 76.4 degrees, and the glycerol contact angle did not change significantly from the original value of 58.0 degrees.

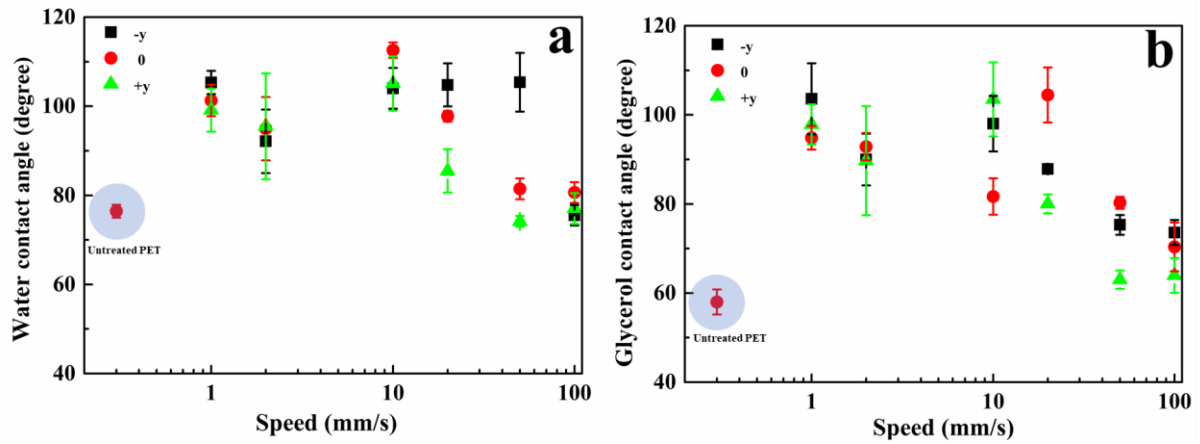

Fig. 6. Distributions of contact angles at positions –y, 0, and +y. (a) deionized water, (b) glycerol (gap: 2.0 mm, exposure: once, MR value: 0.90 %, He flowrate: 29 SLM). The contact angles for the untreated PET are also plotted in each figure.

The flowrate of OFB was increased from 0.131 SLM to 0.262 SLM with a fixed He flowrate of 29 SLM, and the similar experiment was carried out (MR value: 0.90 %). The results of the measured contact angles are summarized in Fig. 6. The uniformity of the treatment was generally improved, compared with the results in Fig. 5. At higher speeds, the contact angle approaches the values of the untreated PET films.

Table 1. XPS elemental analysis of the PET films (gap: 2.0 mm, exposure: once, MR value: 0.90 %).

Speed (mm/s)	*Position*	*Atomic content (at.%)*			*Contact angle (°)*	
		C	F	O	Water	Glycerol
-	-	75.8	0.0	24.2	76.4 ±1.5	58.0± 2.8
1	-y	45.5	52.4	2.1	105.3 ±2.6	103.6± 8.0
	0	48.5	25.6	26.0	101.3 ±3.5	94.9± 2.7
	+y	36.6	36.6	26.8	99.1 ±4.8	97.8± 4.5
10	-y	45.5	39.9	14.6	104.8 ±4.6	98.0± 6.2
	0	55.2	13.2	31.6	112.6 ±1.8	81.7± 4.1
	+y	52.9	17.5	29.6	105.1 ±6.1	103.5± 8.3

XPS measurements were carried out to analyze the elemental composition of the PET film surfaces before and after the plasma treatments. Table 1 summarizes the results XPS together with contact angles. The plasma conditions were the same as those in Fig. 6, and the moving speed was 1 or 10 mm/s. The

untreated PET film surface was dominated by carbon (C) and oxygen (O) atoms without fluorine (F) atoms. After each treatment, F atoms bonded with C were introduced at the surfaces. The F content on the film surfaces tended to be higher at the slower speed. Compared with the "0" and "+y" positions, the F content at the "-y" position was significantly higher at each speed. Specifically, the F content of the film was 52 at.% when the speed was 1 mm/s. At the "0" and "+y" positions, the O content was higher than the untreated one. In other words, both fluorination and oxidation simultaneously occurred at these positions.

4. Discussion

The discharge mode of the DBD is discussed by comparing the visual observation of the plasma in Fig. 2 with the voltage current waveforms in Fig. 3. The overall deformation in the current waveform from the sinusoidal feature suggests an increase in the electrical impedance by the generation of a bulk plasma, while the complex spiky current waveform indicates formation of filamentary micro-discharges, which agrees with the observation of the DBD in Fig. 2.

Measurement of wetting characteristics gives direct indication of surface treatment effects. Fig. 4 (a,b) indicates that the DBD treatment could effectively increase the hydrophobicity of the PET surfaces when the gap was 0.6 mm. On the other hand, when the gap was 2.0 mm, the surfaces did not show hydrophobicity when the He flowrate was lowered as shown in Fig. 4 (c,d). The results demonstrate that the electrode gap has a great impact on the treatment effect. Furthermore, it is suggested that oxidation and/or etching on the PET film surfaces would take place with the gap of 2.0 mm. When the gap becomes larger, the gas flowrates should be increased to account for extra leakage.

The measured result in the unevenness of the wettability shown in Fig. 5 can be related to the uniformity of the gas mixture in the DBD. The photo in Fig. 2 was captured in the same condition. The intense photoemission at "+y" position indicates the lower OFB content in that region. It can be due to insufficient gas mixing process of He and OFB, or uneven local consumption of OFB. It is therefore worth increasing the flowrate of OFB or the MR value as demonstrated in Fig. 6. The result confirms that the treatment can be more uniform by the higher MR value at the high He flowrate.

It is interesting to compare the XPS result with the result of the contact angle measurement in Table 1. It seems that the measured contact angles would be rather insensitive against the significant difference of the F and O contents at different positions. One possible explanation of the discrepancy is that each position would be sufficiently fluorinated to be hydrophobic, and that the differences of the F and O contents may not necessarily affect the contact angles. However, additional investigation will be necessary for further improving the uniformity of the plasma treatment.

5. Conclusion

An air-to-air DBD plasma in a He/OFB gas mixture can introduce fluorine and promote hydrophobicity of the PET films. The flowrates of the gases and the gap of the electrode played important roles for the treatment effects, attributed to the gas content in the plasma. The measured wetting characteristics of hydrophobicity was rather insensitive to the difference in elemental composition of the PET surfaces. The technique presented can be used for continuous air-to-air surface modification of sheet-like specimens including glass fibre fabrics, indicating industrial feasibility of the technology for fibre composite manufacturing.

Acknowledgements

The DACOMAT project has received funding from the European Union's Horizon 2020 research and innovation programme 5 under GA No. 761072. Cheng Fang's work was supported by the Harbin Institute of Technology Scholarship Fund. Research technician Jonas Kreutzfeldt Heininge is acknowledged for design and construction of the air-to-air DBD.

References

[1] Information on https://www.sintef.no/projectweb/dacomat/ "DACOMAT - Damage Controlled Composite Materials". The European Union's Horizon 2020 research and innovation programme under GA No. 761072. Coordinator: SINTEF, Norway. The website inspected on 24th August 2020.
[2] Rask M, Sørensen B F 2012 Eng. Fract. Mech. **96** 37–48
[3] Goutianos S, Sørensen B F 2016 Eng. Fract. Mech. **151** 92–108
[4] Cederløf D J H, Fæster S, Kusano Y 2020 J. Adhesion **96** 2-12
[5] Kusano Y, Cederløf D J H, Fæster S 2020 Key Eng. Mater. **843** 159-164
[6] Kogoma M, Kusano M, Kusano Y 2011 Nova Science Publishers
[7] Kusano Y 2014 J. Adhesion **90** 755-777
[8] Kogelschatz K U 2003 Plasm. Chem. Plasm. Proc. **23** 1-46
[9] Mortensen H, Kusano Y, Leipold F, Rozlosnik N, Kingshott P, Sørensen B F, Stenum B, H Bindslev 2006 J. Appl. Phys. **45** 8506-8511
[10] Lee B J, Kusano Y, Kato N, Horiuchi T, Koinuma H 1997 Jpn. J. Appl. Phys. Pt **36** 2888-2891
[11] Fridman A, Nester S, Kennedy L A, Saveliev A, Mutaf-Yardimci O 1999 Prog. Energy Combustion Sci **25** 211–231
[12] Zhu J J, Ehn A, Gao J L, Kong C D, Aldén M, Larsson A, Salewski M, Leipold F, Kusano Y, Li Z S 2017 Optics Express **25** 20243-20257
[13] Kusano Y, Berglund L, Aitomäki Y, Oksman K, Madsen B 2016 Mater. Sci. Eng. **139** 012027
[14] Kusano Y, Salewski M, Leipold F, Zhu J J, Ehn A, Li Z S, Aldén M 2014 Eur. Phys. J. D **68** 319
[15] Kusano Y 2009 Surf. Eng. **25(6)** 415-416
[16] Zhu J J, Gao J L, Ehn A, Aldén M, Li Z S, Larsson A, Kusano Y 2017 Phys. Plasmas **24** 013515
[17] Kusano Y, Zhu J J, Ehn A, Li Z S, Aldén M, Salewski M, Leipold F, Bardenshtein A, Krebs N 2015 Surf. Eng. **31(4)** 282-288
[18] Teodoru S, Kusano Y, Rozlosnik N, Michelsen P K 2009 Plasm. Proc. Polym. **6** S375-S381
[19] Kusano Y, Andersen T L, Michelsen P K 2008 J. Phys. Conf. Ser. **100** 012002
[20] Mittal K L 1977 Polym. Eng. Sci. **17** 467-473
[21] Kusano Y, Yoshikawa M, Naito K, Okazaki S, Kogoma M 1994 SPSM **7** 77-81
[22] Kusano Y, Madsen B, Berglund L, Oksman K 2019 Celulose 26 7185-7194